Available online at www.sciencedirect.com

Catalysis Today 89 (2004) 169–176

www.elsevier.com/locate/cattod

Microwave plasma assisted preparation of disperse chromium oxide supported catalysts
Influence of the microwave plasma treatment on the properties of the supports

A. Dittmar*, H. Kosslick, D. Herein

Institute of Applied Chemistry Berlin, Adlershof e.V., Richard-Willstätter-Str. 12, D-12489 Berlin, Germany

Abstract

Microwave plasma technology has been used for the deposition of catalytic active chromia species on zirconia and lathanum-doped zirconia supports. The long time microwave (MW) plasma treatment causes a permanent decarboxylation as well as dehydroxylation of the surfaces of support particles. The dehydroxylation leads to a permanent decrease of the number of OH-groups available for anchoring of catalytic active species. This hydrophobization of the surface is also not reversible in humid air. At low or medium MW power and shorter treatment times, as used for microwave plasma enhanced chemical vapour deposition (MPECVD) mediated decomposition–precipitation of catalytic precursors, the surface chemical properties of supports are nearly unchanged. From this point of view, the microwave plasma and radiation should have no negative effect on the plasma chemical preparation of supported catalysts.

Keywords: MPECVD; Microwave plasma; Zirconia; Lanthanum-doped zirconia

1. Introduction

1.1. Supported chromium

Chromium oxide containing catalysts are very important catalysts in chemical and fine chemical industry [1–3]. They have found wide application in numerous polymerisation, oxidation, hydrogenation, dehydrogenation, isomerization, dehydrocyclization aromatisation as well as DENOx reactions. This catalytic diversity is due to the variability of the valence state of chromium as well as due to the different molecular structures of the supported chromium oxides. Beside silica and aluminium oxide, zirconia or modified zirconium dioxide has been advantageously used as catalyst support [4,5]. The valence states and the molecular structure of the supported chromium species depend on the applied preparation procedure as well as on the physico-chemical nature of the support.

Doping of zirconia with other elements is of importance because it stabilizes the catalytic interesting tetragonal or cubic zirconia phases. These phases exhibit increased specific surface areas and contain a higher number of oxygen vacancies. The latter can be involved directly in the catalytic reaction or allow additional anchoring of catalytically active species. The doting with lanthanum increases the ion conductivity as well as the acid–base properties of the support.

Usually, chromium support catalysts are prepared by wet chemical procedures and are environmentally not friendly because of the unavoidable existence of poisonous Cr^{6+} compounds and the necessity of solvents. Low-temperature plasma chemical preparation of supported chromia catalysts offers an environmentally more friendly procedure as formation of hazardous waste solutions is diminished. Thus, the applications of the low-temperature microwave plasma could be of special interest for the preparation of supported nano-sized metal oxides, because aggregations caused by thermal treatment might be avoided. Narrower particle size distributions are expected in comparison with conventional preparation methods, e.g. by wet impregnation. Therefore, this method is an interesting alternative for non-conventional preparation of highly disperse, i.e. nano-structured supported catalysts [6].

This paper deals firstly with the influence of the microwave plasma treatment on the textural, structural and

---

* Corresponding author. Tel.: +49-30-6392-4230; fax: +49-30-6392-4350.

E-mail address: dittmar@aca-berlin.de (A. Dittmar).

0920-5861/$ – see front matter © 2003 Elsevier B.V. All rights reserved.
doi:10.1016/j.cattod.2003.11.023

surface chemical properties of zirconia and lanthanum-doped zirconia supports. A further publication over the results for plasma chemical preparation of chromia supported on zirconia and lanthanum-doped zirconia will follow.

2. Experimental

2.1. Preparation of supports

Zirconia (ZrO_2) and lanthanum-doped zirconia (La_2O_3–ZrO_2) were used as supports for catalytic active components. The supports were prepared by calcination of commercially available $Zr(OH)_4$ and $La(OH)_3/Zr(OH)_4$ (MEL) at 873 K in air. For this, the zirconium hydroxide was heated stepwise at different heating rates to the required temperature and hold at that temperature for a certain time until heating was continued. The following temperature regime was used:

(1) 30 K/min to 573 K, 1 h isotherm;
(2) 10 K/min to 673 K, 0.5 h isotherm;
(3) 10 K/min to 773 K, 0.5 h isotherm;
(4) 10 K/min to 875 K, 4 h isotherm.

Then the samples were allowed to cool down to room temperature. The specific surface area of zirconia was 33 m^2/g and of lanthanum-doped zirconia was 90 m^2/g [7]. The lanthanum content checked by ICP was 1.6 mol%.

2.2. Microwave plasma treatment

A Siemens microwave plasma chamber has been used for detecting the influence of microwave plasma treatment on the properties of zirconia and lanthanum-doped zirconia. The used vacuum recipient has a volume of about 50 l and could be evacuated up to 5 Pa. A flask of quartz mounted on a metallic rod was placed into the recipient. A 2.46 GHz magnetron together with a power supply was used for the generation of microwaves. The powdery catalyst supports were placed into the quartz flask, which was rotated during the treatment. Thereafter, the chamber was evacuated to 5 Pa and the plasma gas flow was tuned with a mass flow controller. The pressure of the plasma gas was controlled with a baratron. Oxygen was used as feed gas. The applied microwave power was set on 100–500 W. After micowave plasma enhanced chemical vapour deposition (MPECVD) treatment samples were removed and characterized in order to study the influence of the different treatment conditions on the state of the catalyst supports.

2.3. Characterization

The textural properties as specific surface area, pore volume, pore size were determined by nitrogen adsorption. Nitrogen adsorption and desorption isotherms were recorded on commercial gas adsorption system ASAP 2000 M (Micromeritics). Before measurement, samples of ca. 50 mg were activated by heating in vacuum to 373 K for 12 h until constant pressure. Sorption measurements were carried out at liquid nitrogen temperature. The specific surface area was determined after Brunauer, Emmet and Teller (BET) [7]. The pore sizes and volumes were determined using the BJH method [8].

The X-ray diffraction (XRD) powder patterns were recorded on a STOE SADI P diffractometer using Cu Kα_1 radiation. The diffraction patterns were recorded with a position sensitive detector (PSD). The broadenings and shifts of reflections were determined by using silicon samples as reference material.

The laser Raman spectra were measured on a DILOR-XY Raman spectrometer. For excitation an argon ion laser (ILA 120, CZ Jena) operating at 488 and 514.5 nm (1–10 mW power) as well as a helium–neon laser (HNA 188, CZ Jena) operating at 632.8 nm was used. Raman spectra were recorded in the spectral range between 100 and 1300 cm^{-1}. FT-IR spectra in the KBr technique were measured with a Nicolet Magna 500 spectrometer. The spectral resolution was 4 cm^{-1}. The sample to KBr ratio was 1:100–200. In situ measurements were carried out on a FTS-60 spectrometer (Bio-Rad) using a heatable IR vacuum cell on self-supporting wafers. Prior measurements sample were activated either for 10 min at 313 K or for 60 min at 873 K in an 20 vol.% oxygen–helium stream. Thereafter, samples were evacuated for 30 min and cooled down to 313 K. The spectra were collected at 313 K coadding 256 scans at a resolution of 2 cm^{-1}. For semi-quantitative measurements, band intensities were normalized to the sample weight per surface unit.

Combined TG/DTA–MS measurements in the temperature range between 298 and 1073 K were carried out on a Perkin–Elmer DSC 7 thermoanalysis system in air or helium. The heating rate was 10 K/min. The sample weight was ca. 25 mg. A quadrupole mass spectrometer (Micromass PC, VG Quadrupoles) was used for continuous mass spectrometric analysis of the desorbed products at the masses $m/e = 18$ (water), 28 (carbon monoxide) and 44 (carbon dioxide).

For chemical analysis of samples the inductive coupled plasma optical emission spectrometry (ICP-OES) was applied (Perkin–Elmer Optima 3000XL).

3. Results and discussion

3.1. Calcined supports

3.1.1. Zirconia

In order to obtain information about the influence of the MW plasma treatment on the structural, textural and surface chemical properties the materials were characterized before and after treatment in more detail. Structural properties were investigated using XRD and Raman spectroscopy. Textural properties were analysed by nitrogen sorption measurements. Changes of surface chemical properties were checked

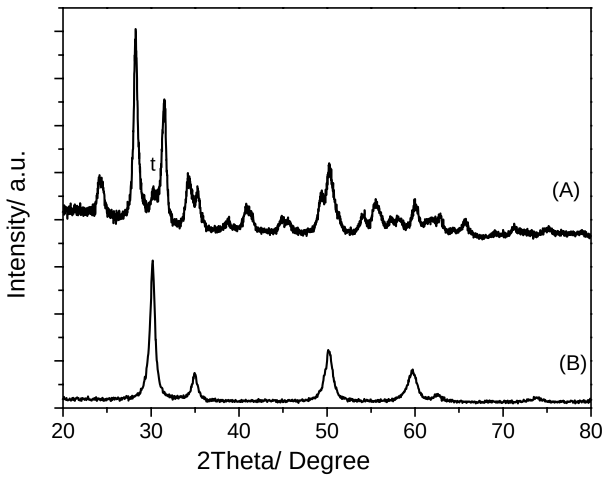

Fig. 1. X-ray powder diffraction of (A) m-ZrO_2 with a fraction of tetragonal phase (t) and (B) $La_{0.1}Zr_{0.9}O_{1.95}$ (calcined at 873 K).

by FT-IR spectroscopy and coupled TG/DTA–MS measurements.

The XRD pattern confirms that the thermodynamic stable monoclinic zirconium dioxide phase (m-ZrO_2) is obtained after calcinations of the zirconium hydroxide precursor at 873 K (Fig. 1A). Beside the reflections typically observed with m-ZrO_2 an additional reflection at $2\Theta = 30.2^\circ$ appears in the diffraction pattern. It points to the presence of some cubic (c) or tetragonal (t) ZrO_2 in sample. The volume fraction of these impurity was determined using the Gravie–Nicholson relation and amounts to 0.13 [9,10]. Both, the c-ZrO_2 and the t-ZrO_2 phase, show a reflection near at $2\Theta = 30.2$. Therefore, both the phases are hardly to be distinguished by XRD. However, the Raman spectrum reveals that the additional phase belongs to t-ZrO_2 (Fig. 2A). In addition to the Raman bands of m-ZrO_2, Raman bands appear at 145 and 267 cm^{-1} [11] clearly indicating the presence of the tetragonal phase. Cubic ZrO_2 shows a characteristic intensive Raman band at 490 cm^{-1} only (compare Table 1). The volume fraction of t-ZrO_2 in m-ZrO_2 was determined from the intensity ratio of the Raman bands of m-ZrO_2 (177 and 189 cm^{-1}) and t-ZrO_2 (145 and 267 cm^{-1}), respectively, using again the Gravie–Nicholson relation. The obtained value of 0.15 agrees well with the XRD results.

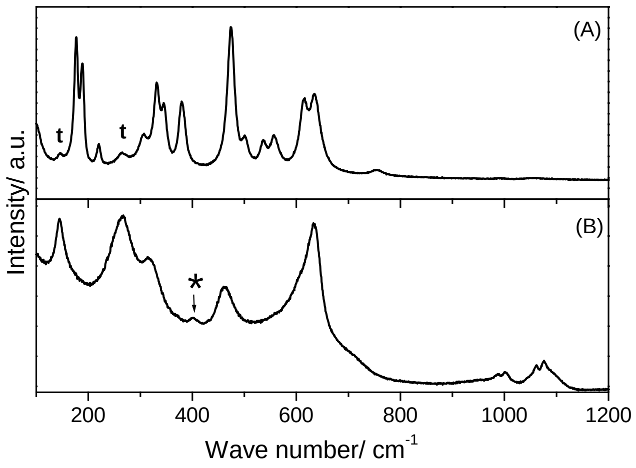

Fig. 2. Raman spectra of (A) m-ZrO_2 with a fraction of tetragonal phase (t) and (B) $La_{0.1}Zr_{0.9}O_{1.95}$ with a fraction of La_2O_3 (*) (calcined at 873 K).

Table 1
Typical vibration modes in Raman spectra for m-, t- and c-ZrO_2 (sh) shoulder

Wave number (cm^{-1}) m-ZrO_2	Wave number (cm^{-1}) t-ZrO_2	Wave number (cm^{-1}) c-ZrO_2
158.0	145.9	490
177.4	267.1	
189.5	315.1	
221.4	456.0	
306.0	607.1 (sh)	
332.5	644.5	
346.6		
381.1		
474.6		
500.2		
537.1		
557.9		
615.2		
637.6		

3.1.2. Lanthanum-doped zirconia

As expected after calcination of the La-doped precursor the tetragonal phase is obtained (Figs. 1B and 2B). As generally known, substitution of lattice Zr^{4+}-cations by La^{3+}-cations leads to the formation of at meta stable tetragonal or cubic zirconia phase with the composition $La_{0.1}Zr_{0.9}O_{1.95}$ at room temperature. As the XRD pattern of cubic and tetragonal ZrO_2 are very similar, the presence of t-ZrO_2 has been confirmed on the basis of its characteristic Raman spectrum (Fig. 2B). An additional weak signal at 402 cm^{-1} indicates that the sample contains La_2O_3. The broad Raman bands appearing between 950 and 1150 cm^{-1} belong to the presence of surface carbonate species [12], which are not clearly seen in the Raman spectrum of ZrO_2. But this might be due to the distinct lower specific surface area of ZrO_2 and, hence, lower concentration of carbonate species in the ZrO_2 do to smaller basicity of ZrO_2 in comparison to the La-doped sample. The formation of lanthanum carbonate species from lanthanum not incorporated in the zirconia lattice also cannot be excluded.

Doting of ZrO_2 results also in a decrease of the crystallite size of primary particles from 400 to 100 Å [13], which is in line with the found increase in the specific BET surface area (Table 2).

The nitrogen adsorption–desorption isotherms and the pore size distribution of m-ZrO_2 and $La_{0.1}Zr_{0.9}O_{1.95}$ are shown in Figs. 3 and 4. The isotherms are belong to the type IV according to the IUPAC nomenclature [14] and are

Table 2
Textural parameters of m-ZrO_2 and $La_{0.1}Zr_{0.9}O_{1.95}$ supports

Support	S_{BET} (m^2/g)	V_P (cm^3/g)	D_P (Å)	D (Å)
m-ZrO_2	33	0.13	80	400
$La_{0.1}Zr_{0.9}O_{1.95}$	89	0.097	32	100

S_{BET}: specific surface area; V_P: specific pore volume; D_P: pore size; D: crystallite size.

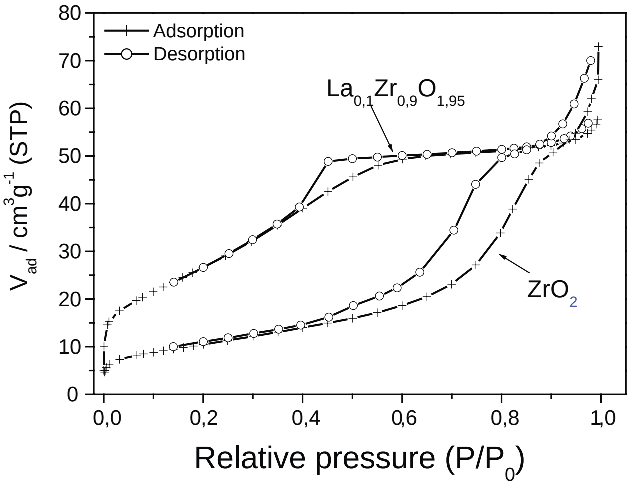

Fig. 3. Nitrogen adsorption–desorption isotherm for m-ZrO_2 and $La_{0.1}Zr_{0.9}O_{1.95}$ at 77 K.

typically found with mesoporous materials exhibiting strong interaction with the adsorbate. The La-doped sample has a higher specific surface area, pore volume and pore size as the non doped zirconia (Table 2 and Fig. 4). The H1 type hysteresis of m-ZrO_2 is typically found with agglomerated spherical uniform particles. The H2 type hysteresis of the La-doped zirconia is assigned to bottle-necked pores. So, both the supports are mesoporous but show different pore sizes and surface areas due to different morphology of the primary particles.

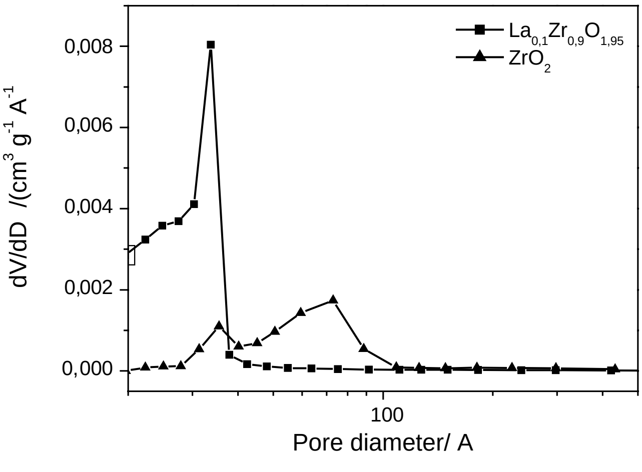

Fig. 4. Pore size distribution of ZrO_2 and $La_{0.1}Zr_{0.9}O_{1.95}$.

3.2. Long time oxygen MW plasma treated supports

In order to check a possible influence of the MW plasma chemical treatment on the structural, textural or surface chemical properties the calcined supports have been treated for 16 h in an oxygen microwave plasma using a MW power of 200 W and an oxygen partial pressure of 70 Pa.

XRD pattern (here not shown) of the plasma treated m-ZrO_2 and La-doped t-ZrO_2 supports are nearly unchanged with respect to the calcined non-plasma treated samples. This indicates that the plasma treatment does not lead to phase changes in the bulk.

3.3. Raman spectroscopy

3.3.1. m-ZrO_2

The corresponding Raman spectra of MW plasma treated samples are shown in Fig. 5. With ZrO_2 an additional Raman band at 1046 cm^{-1} is observed, which is due to the formation of surface carbonate species after plasma treatment. The formation of surface carbonate species points to an increased reactivity of the surface after plasma treatment and subsequent up-take of carbon dioxide after exposure to air. The Raman bands of framework vibrations of m-ZrO_2 before and after plasma treatment are unchanged.

3.3.2. $La_{0.1}Zr_{0.9}O_{1.95}$

In contrast, the Raman spectrum of La-doped zirconia shows after oxygen plasma treatment additional Raman bands at 177, 189 and 381 cm^{-1} which can be assigned to m-ZrO_2 (Fig. 6). The volume fraction of m-ZrO_2 in the tetragonal La-doped zirnonia phase is 0.023 according to the intensity ratios of the corresponding Raman bands. It is assumed, that the starting material already contains some m-ZrO_2, which recrystallizes under the influence of the MW radiation leading to more resolved Raman bands. Interestingly, the Raman bands of surface carbonate species

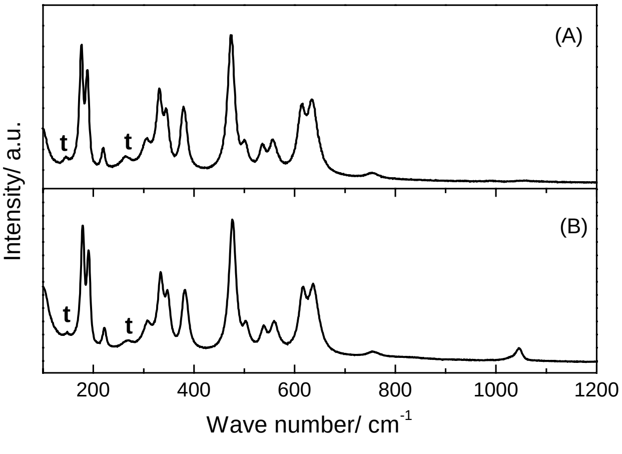

Fig. 5. Raman spectra of (A) m-ZrO_2 and (B) m-ZrO_2 with subsequent oxygen plasma treatment with a low fraction of t-ZrO_2 (t), respectively, m-ZrO_2 was obtained by calcination of zirconiumoxohydroxide at 873 K.

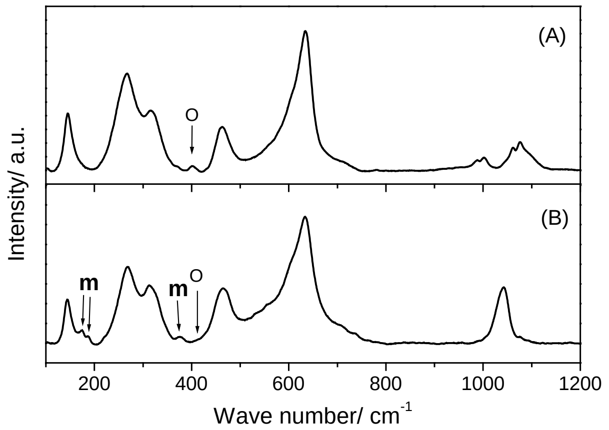

Fig. 6. Raman spectra of (A) $La_{0.1}Zr_{0.9}O_{1.95}$ with a low fraction of (o) La_2O_3 and (B) $La_{0.1}Zr_{0.9}O_{1.95}$ with subsequent oxygen plasma treatment with a low fraction of m-ZrO_2 (m), respectively, and (o) La_2O_3; $La_{0.1}Zr_{0.9}O_{1.95}$ was obtained by calcination of La-doped zirconiumoxohydroxide at 873 K.

observed between 900 and 1150 cm^{-1} disappear after long time plasma treatment. Instead a new Raman band at 1046 cm^{-1} appears indicating the change of the nature of the surface carbonates [15] (Table 3).

Table 3
Allocation of vibration modes of surface carbonate species and formiate observed in FT-IR spectra of m-ZrO_2 and $La_{0.1}Zr_{0.9}O_{1.95}$ (after calcination at 873 K and afterwards treatment in vacuum at 313 K). The FT-IR measurements were carried out at 313 K in vacuum

Wave number (cm^{-1}) m-ZrO_2	Wave number (cm^{-1}) $La_{0.1}Zr_{0.9}O_{1.95}$	Vibration modes
Hydrogen carbonate		
1625	1625	as-$\nu_{C=O}$ (asymmetric C=O-stretch vibration)
1430	1430	s-$\nu_{C=O}$ (symmetric C=O-stretch vibration)
1225	1225	δ_{OH} (OH-deformation vibration)
Monodentate carbonate		
1490		as-$\nu_{C=O}$ (m-ZrO_2)
1390		s-$\nu_{C=O}$ (m-ZrO_2)
1442	1450	as-$\nu_{C=O}$ (t-ZrO_2)
1423	[a]	s-$\nu_{C=O}$ (t-ZrO_2)
Bidentate carbonate		
1575	1550	as-$\nu_{C=O}$
1560	[b]	as-$\nu_{C=O}$[c]
1335	1355	s-$\nu_{C=O}$
1325	[b]	s-$\nu_{C=O}$[c]
Bidentate carbonate		
1430[b]	1430[b]	$\nu_{C–O}$
Formiate		
1560	1581	as-$\nu_{O–C–O}$
1380	1382	δ_{CH}
1368	1368[a]	s-$\nu_{O–C–O}$

[a] Modes not resoluted.

[b] Existence cannot be excluded.

[c] Existence of bidentate carbonate species of different geometric configuration and/or on different crystal surface areas.

Both calcined supports contain after calcination ca. 0.5 wt.% of residual carbon, which can be oxidized in the oxygen plasma forming different anchored carbonates or formiates. Therefore, FT-IR spectra in the range of the carbonyl valence vibration between 1100 and 1800 cm^{-1} have been recorded in order to get more detailed information on the nature of these species.

3.4. FT-IR spectroscopy

In the FT-IR spectra of calcined m-ZrO_2 and $La_{0.1}Zr_{0.9}O_{1.95}$ samples are observed broad structured absorbances between 1750 and 1200 cm^{-1} showing the presence of a variety of different surface carbonate species like mono and bidentate, bridged bidentate, or multidentate carbonates as well as of formiate (Figs. 7 and 9) [16,17].

3.4.1. m-ZrO_2

The calcined ZrO_2 contains hydrogen carbonate species indicated by the weak bands (shoulders) at 1625 (as-$\nu_{C=O}$) and 1225 cm^{-1} (δ_{OH}) (Fig. 7). The corresponding s-$\nu_{C=O}$ vibration band is overlapped by intense vibrations of uni-dendate carbonate occurring at 1442 and 1423 cm^{-1} [17–19]. The vibration bands at 1490 and 1390 cm^{-1} (weak) as well as 1450 and 1425 cm^{-1} (strong) can be assigned to monodentate carbonates bound to m- and t-ZrO_2, respectively, [20]. The shift of band positions is assigned to the different geometry of the oxygen surface of the two crystalline modifications [20,21]. This finding supports the presence of some tetragonal zirconia in m-ZrO_2 support. The vibration bands near 1575 (as-$\nu_{C=O}$) and 1325 cm^{-1} (s-$\nu_{C=O}$) are assigned to bidentates [18–20]. These bands can also be split if bound to different modifications giving rise to the appearance of additional vibration bands

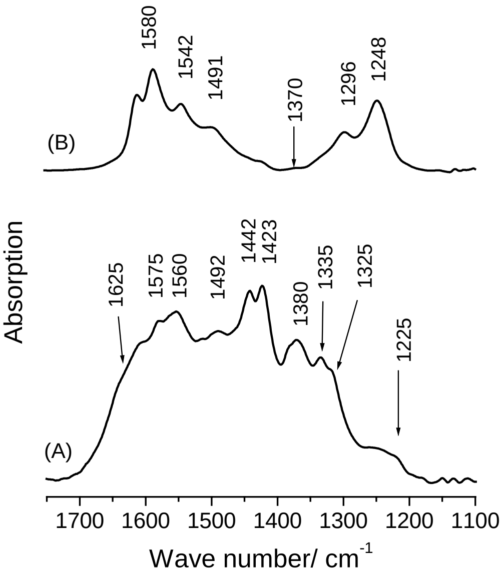

Fig. 7. In situ FT-IR spectra of calcined m-ZrO_2 before (A) and after oxygen plasma treatment (B).

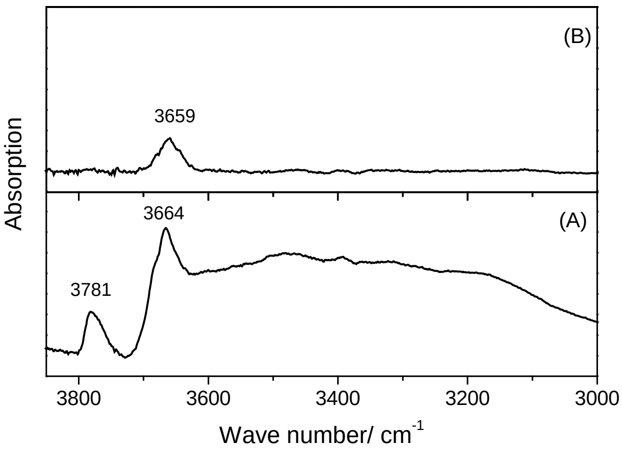

Fig. 8. OH-group vibration spectrum of dehydrated (A) and oxygen MW plasma treated m-ZrO_2 (B).

at 1560 and 1335 cm^{-1}, respectively. The vibration bands at 1580, 1380 and 1368 cm^{-1} are due to formiate species [22]. The band at 1639 cm^{-1} (δ_{OH}) is due to physically adsorbed water. The latter is confirmed by the OH-vibration spectrum (Fig. 8A). After oxygen plasma treatment, the thermodynamically less stable hydrogen and monodentate carbonate species are nearly completely removed (Fig. 8B). This shows the occurrence of distinct changes in the surface chemical properties during oxygen plasma treatment.

The latter is also reflected in the corresponding OH stretching vibration spectra (Fig. 7). After MW plasma treatment the vibration band at 3781 cm^{-1} (stretching vibration of the OH_I group of two-fold coordinated lattice oxygen atoms) disappears and the intensity of the vibration band near 3664 cm^{-1} (stretching vibration of the OH_{II} group of three-fold coordinated lattice oxygen atoms) distinctly diminishes [21]. Only one absorbance located at 3659 cm^{-1} remains after plasma treatment. These changes remain stable also after exposure of the samples to ambient air. Hence, the plasmachemically treated surface of zirconia behaves more hydrophobic. This supports earlier conclusions from Jacob et al. [21] of a possible structural change of the external surface structure of the m-ZrO_2 support from a monoclinic to a cubic/tetragonal state or to partial formation of an amorphous surface area.

3.4.2. $La_{0.1}Zr_{0.9}O_{1.95}$

The observed broad absorbance in the range of carbonyl vibration is less resolved than found with m-ZrO_2 (Fig. 9A). This might be due to the additional presence of La_2O_3 as shown by the Raman spectra. Lanthanum oxide forms also carbonate species of different origin. Their vibration bands overlap strongly with those of zirconia carbonate species [23,24]. Vibration bands of mono and bidentate carbonate species of lanthanum oxide arise at 1490–1415 and 1560–1360 cm^{-1}, respectively. Vibration bands at 1540, 1475, 1400 and 1330 cm^{-1} belong to $La_2O_2CO_3$ dioxomonocarbonate. Therefore, a detailed band assignment can hardly be obtained. Some hydrogen carbonate is found indicated by the weak shoulders arising at 1625 and 1225 cm^{-1}, which might be due to the presence of some m-ZrO_2 in the sample as confirmed by the Raman spectra shown above. The bands near 1550 and 1355 cm^{-1} are assigned to excitation of as-$\nu_{C=O}$ of two slightly different bidentate carbonate, most likely corresponding to two slightly different geometrical configurations and/or different crystal planes [20]. The bands near 1430 and 1581, 1382 and 1370 cm^{-1} show the presence of monodentate carbonate and of formiate species, respectively.

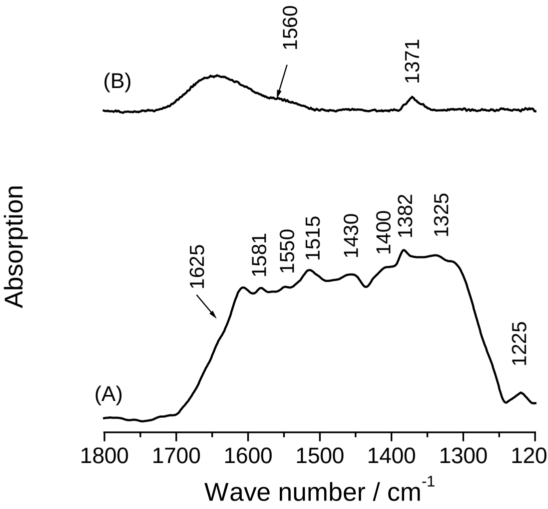

Fig. 9. In situ FT-fIR spectra of dehydrated $La_{0.1}Zr_{0.9}O_{1.95}$ before (A) and after oxygen plasma treatment (B) in the range of carbonyl vibrations.

After oxygen MW plasma treatment the surface carbonate species are nearly completely removed (Fig. 9B). Only weak absorbances are found near 1650 cm^{-1} (δ_{OH} of coordinatively bound water) and 1371 cm^{-1} (formiate species). In OH-vibration spectrum of $La_{0.1}Zr_{0.9}O_{1.95}$ only a single OH stretching mode at 3669 cm^{-1} appears (Fig. 10A), which is assigned to isolated OH_{II} groups. As observed with m-ZrO_2

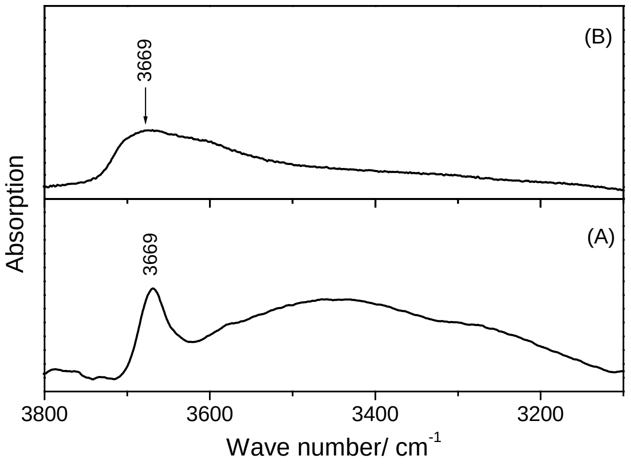

Fig. 10. OH-group vibration spectrum of dehydrated (A) and oxygen MW plasma treated $La_{0.1}Zr_{0.9}O_{1.95}$ (B).

oxygen MW plasma treatment leads to a dehydroxylation of the surface (Fig. 10B). The OH_{II} band is broadened. Obviously, the plasma treatment leads to a higher degree of disorder in the surface of the support (amorphous surface structure). That means, OH-groups of different bonding strength can develop and/or false arranged t- or also small portions of m-ZrO_2. Again, after plasma treatment the surface behaves more hydrophobic.

3.4.3. *Thermoanalysis*

The decomposition and desorption of surface species was also followed by TG–MS. The observed total losses of calcined m-ZrO_2 and $La_{0.1}Zr_{0.9}O_{1.95}$ at 1100 K belong to 1.4 and 4.8 wt.%, respectively. These different weight losses are in line with the different BET surface areas of these supports. The greatest loss is observed after heating to 473 K. In this temperature range namely water and carbon dioxide from the decomposition of hydrogen carbonates are found by MS analysis as desorption products. Between 473 and 1073 K mainly desorption of carbon dioxide is detected originating from the decomposition of the different surface carbonate. With m-ZrO_2 desorption of carbon dioxide is finished at 800–900 K. Whereas with $La_{0.1}Zr_{0.9}O_{1.95}$ desorption of carbon dioxide occurs in steps ranging 473–750 K and at higher temperature ranging from 750 to 1073 K. These results agree with the FT-IR observation of different bound surface carbonate complexes in both types of supports.

After plasma treatment, only some water is desorbed up to a temperature of 473 K but nearly no carbon dioxide. The hydrogen carbonates have been decomposed during plasma treatment. The surface structure has been changed and does not allow the formation of new hydrogen carbonates during contact with air. The water content is also diminished. The changes in the surface chemical properties found after plasma treatment (e.g. increased hydrophobity) are maintained also after storage of samples for 6 months in air.

3.4.4. *Short time microwave plasma treatment*

After short time treatment of the supports in the oxygen plasma for 1 h at a microwave power of 200 W and an oxygen pressure of 130 Pa no changes of surface chemical properties could be detected by FT-IR spectroscopy. Therefore, at conditions of usual plasma chemical decomposition of catalytic precursors surface properties of the zirconia supports remain nearly unchanged. However, with increasing of MW power to 500 W decarboxylation of the support surface is observed (Fig. 11). Under these more severe conditions, changes in the surface chemical properties cannot be excluded.

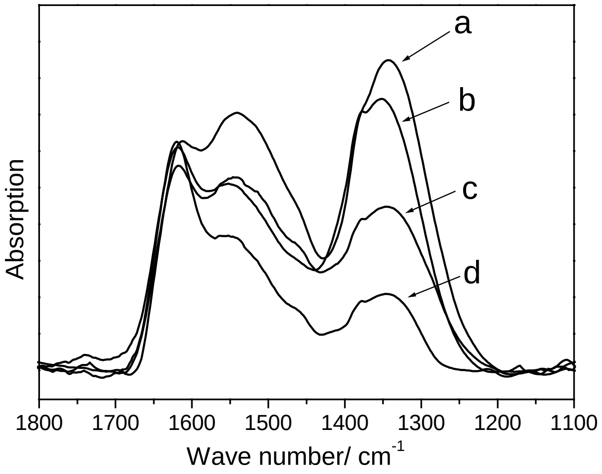

Fig. 11. FT-IR spectra of $La_{0.1}Zr_{0.9}O_{1.95}$ before (a) and after 1 h oxygen plasma treatment at 100 Pa and (b) 300 W, (c) 400 W and (d) 500 W (KBr waver).

4. Conclusions

At the plasma chemical preparation of supported catalysts also the influence of plasma that means especially the influence of active species and/or plasma radiation as well as of microwave radiation on surface area chemical properties of supports are of great interest. Thus, the characterisation of supports before and after plasma treatment was carried out. The detailed comparison of the textural, structural and surface chemical properties of calcined and microwave plasma treated m-ZrO_2 and $La_{0.1}Zr_{0.9}O_{1.95}$ supports led to the following specified most important results:

- In the case of m-ZrO_2, long time plasma treatment leads to changing in the surface structure accompanied by partially monoclinic to cubic/tetragonal phase transition as well as the generation of a partially amorphous surface area (Fig. 12A).
- With $La_{0.1}Zr_{0.9}O_{1..95}$ the presence of a partially amorphous or c-, t-ZrO_2 defect structure is assumed after long time plasma treatment (Fig. 12B). These changes are stable during long time storage in air at least for 6 months as also with m-ZrO_2.
- The microwave plasma treatment or the microwave radiation can initiate recrystallization processes from before amorphous components.
- Furthermore, the long time MW plasma treatment causes a decarboxylation as well as a dehydroxylation of the surfaces of support particles. The changes of surface chemical properties also occur after shorter treatment times, provide the MW power is substantially increased. At low or medium MW power and shorter treatment times the surface chemical properties of supports are nearly unchanged.

For the catalysts preparation from great importance is the possibility of anchoring the precursor or active component to the support surface area—mostly by reaction with hydroxyl groups. As mentioned before, the plasma treatment leads to dehydroxylation that means to a permanent decrease of the number of OH-groups available for anchoring of catalytic active species. This hydrophobization of the surface is also not reversible in humid air. Like the following [6] and planned publications however show, for MPECVD mediated

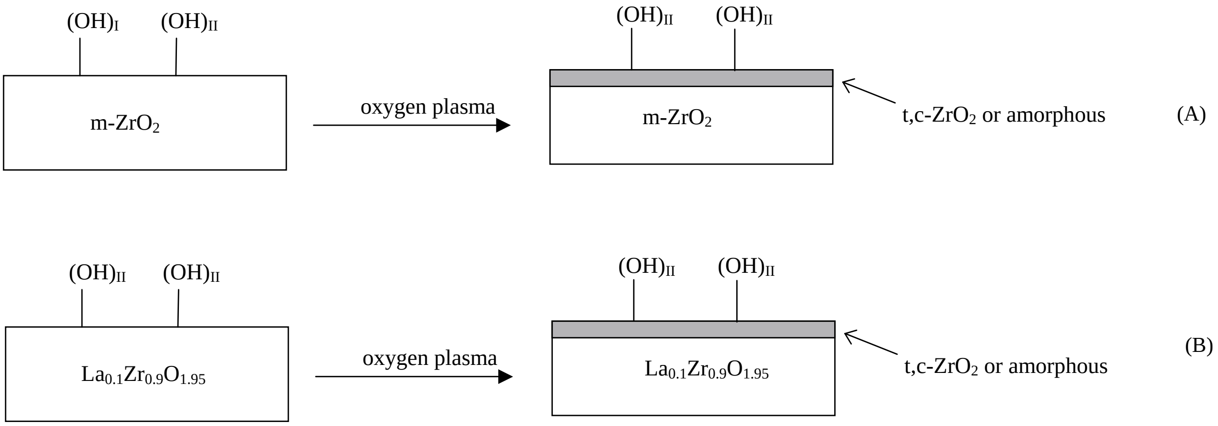

Fig. 12. Microstructure model of surfaces of m-ZrO_2 (A) and $La_{0.1}Zr_{0.9}O_{1.95}$ (B) before and after oxygen plasma treatment.

decomposition–precipitation of catalytic precursors low or medium MW power and shorter treatment times are used. From this point of view, the microwave plasma and radiation should have no negative effect on the plasma chemical preparation of supported catalysts.

Acknowledgements

This work was supported by Federal Ministry of Education and Research (FRG) and the Berlin Department of Science, Research and Culture (No. 03C 3005). The authors thank Prof. Dr. M. Baerns for the support of this work, Dr. M. Schneider (XRD), Dr. Trunschke (FTIR), Dr. Brzezinka (Raman) for helpful discussions and Mrs. Hidde for the plasma chemical preparation of the substances.

References

[1] Ch.P. Poole, D.S. Mac Iver, Adv. Catal. 17 (1967) 223.
[2] M.P. McDaniel, Adv. Catal. 33 (1985) 47.
[3] B.M. Weckhuysen, I.E. Wachs, R.A. Schoonheydt, Chem. Rev. 96 (1996) 3327.
[4] S. De Rossi, G. Ferraris, S. Fremiotti, A. Cimino, V. Indovina, Appl. Catal. A 81 (1992) 113.
[5] N.B. Jackson, J.G. Eckerdt, J. Catal. 101 (1986) 90.
[6] A. Dittmar, H. Kosslick, J.-P. Müller, M.-M. Pohl, Surf. Coat. Technol., submitted for publication.
[7] S. Brunauer, P.H. Emmett, E. Teller, J. Am. Chem. Soc. 60 (2) (1938) 309.
[8] S. Partyka, F. Roquerol, J. Roquerol, J. Colloid Interface Sci. 68 (1979) 21.
[9] H. Toraya, M. Yoshimura, S. Somiya, J. Am. Ceram. Soc. 67 (1984) C119.
[10] H.K. Schmid, J. Am. Ceram. Soc. 70 (1987) 367.
[11] D. Michel, M. Perez, Y. Jorba, R. Collongues, J. Raman Spectrosc. 5 (1976) 163.
[12] D.R. Clarke, F. Adar, J. Am. Ceram. Soc. 65 (1982) 284.
[13] Th.H. De Kreijser, E.J. Mittemeijer, H.C.F. Rozendaal, J. Appl. Cryst. 16 (1983) 309.
[14] K.S.W. Sing, D.H. Everett, R.A.W. Haul, L. Moscou, R.A. Pierotti, J. Rouquerol, T. Siemieniewska, Pure Appl. Chem. 57 (4) (1985) 603.
[15] E. Djurado, P. Bouvier, G. Luczeau, J. Solid State Chem. 149 (2000) 399.
[16] D.A. Fumo, M.R. Morelli, A.M. Segadaes, Mater. Res. Bull. 31 (10) (1996) 1243.
[17] A.A. Tsyganenko, E.A. Trusov, Russ. J. Phys. Chem. 59 (1985) 2602.
[18] W. Hertl, Langmuir 5 (1989) 96.
[19] L.H. Little, Infrared Spectra of Adsorbed Species, Academic Press, New York, 1966.
[20] B. Bachiller-Baeza, I. Rodriguez-Ramos, A. Guerrero-Ruiz, Langmuir 14 (1998) 3556.
[21] K.-H. Jacob, E. Knözinger, S. Benier, J. Mater. Chem. 3 (1993) 651.
[22] D. Bianchi, T. Chafik, M. Khalfallah, S.J. Teichner, Appl. Catal. A: Gen. 105 (1993) 223.
[23] S. Lacombe, C. Geantet, C. Mirodatos, J. Catal. 151 (1994) 439.
[24] B. Klingenberg, M.A. Vannice, Chem. Mater. 8 (1996) 2755.